Theoretical and Experimental Characterization of Moving Wireless Power Transfer Systems

Alex Pacini[1], Franco Mastri[1], Riccardo Trevisan[1,2], Alessandra Costanzo[1], Diego Masotti[1]
[1] DEI – "Guglielmo Marconi"; School of Architecture and Engineering, University of Bologna, Italy
[2] IMA SpA, Bologna, Italy

***Abstract*— The idea of this paper is to develop a moving resonant wireless power transfer (WPT) system capable of keeping the coupling factor, and thus the power transfer, invariable with respect to the reciprocal system sides positions. A typical scenario is the WPT to moving objects on a platform equipped with a sequence of coils underneath. If a single TX coil is active at a time, the receiver movement would cause the coupling coefficient, and consequently the transmitted power, to oscillate. To cope with this problem, in this work we propose to make use of two active Tx coils. Different coil geometries and coil connections have been investigated, trying to get an insight into the coupling mechanism. This have been done by full-wave simulations and measurements of the selected structures and by varying some key parameters of the geometry itself. The connections between coils have been done in post-processing and the results have been plotted for comparison. Future work has been proposed.**

***Index Terms*— WPT, Moving Vehicles, Near-Field.**

I. INTRODUCTION

In the recent literature great interest has been devoted to wireless power transfer (WPT) exploiting resonant coils coupled via their magnetic fields (see e.g. the references in [1]-[2]): the issues of variable distance between the transmitter (Tx) and the receiver (Rx) coils and of coil misalignment have been largely discussed [3]-[6], and the feasibility of WPT systems deploying Rx moving coil has also been demonstrated [7]-[8]. However the conditions a WPT system with sliding coils has to fulfil in order to maintain constant performance on the move are still missing.

With this paper we try to bridge this gap by means of the development of a resonant WPT system capable of keeping the coupling factor as constant as possible by studying the effects of the moving receiving coil. A typical application for such a system is the power transfer to a moving vehicle directly from the pavement, where the coils can be placed underneath.

In order to explain the concept, firstly we start by analyzing the behavior of a traditional setup, with a fixed transmitting coil and a single sliding one. In a second instance, we consider two transmitting coils, with series or parallel connections, and by sliding the movable one over the two fixed coils we investigate again the variations of the coupling factor. This allows to prove that, by properly choosing the Rx coil length it is possible to obtain a constant coupling coefficient during the coil movement.

This second approach can be extended by placing a series of coils along the path of a moving vehicle. While the vehicle is moving, two consecutive fixed coils are kept active. Each pair of coils is kept active from the instant when the axis of the receiver coil is aligned with axis of the first fixed coil, till the instant when it aligns with the second one. A new pair is then formed by deactivating the first coil and activating the coil which precedes the vehicle. Hence, at this point the cycle restarts. In this way it is possible to keep the Rx coil within the region where the coupling coefficient remains constant.

The whole approach is carried out by qualitative/intuitive explanations and confirmed by both full wave simulations and measurements.

II. MOVING COIL ANALYSIS

A. Geometrical structures description

In order to demonstrate the principle of operation of the system, let us consider the simple structure consisting of three coils depicted in Fig. 1. The coplanar coils 2 and 3 are fixed and represent the Tx coils placed in the pavement, while coil 1, which lays on a parallel plane placed at distance *h*, represents the sliding Rx coil. The outlined coil configuration is designed for high power resonant WPT. The adopted support material of the coils is FR4, but any non-magnetic dielectric material would work.

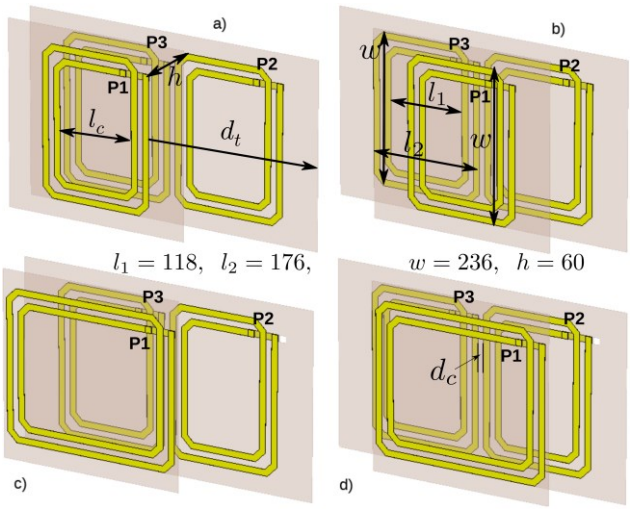

Fig. 1. Examples of planar (moving) Rx coil and couple of (fixed) Tx coils layouts and reciprocal positions.

This system is analyzed by varying the position of the moving coil from the configuration represented in Fig. 1(a), where coil 1 is coaxial with coil 3, to the configuration of Fig. 1(b) where the center of coil 1 is placed midway between the centers of coil 2 and coil 3. Since the Tx coils are assumed to be identical, the behavior of the coupling coefficients during a subsequent moving of the Rx coil, from this position till when it becomes coaxial with coil 2, can be derived by symmetry.

The analysis is repeated for several values of the inner length l_c of the Rx coil, starting from a value equal to the inner length l_1 of the Tx coils, as shown in Fig. 1(a) and (b), to a value of $1.78l_1$, as shown in Fig. 1(c) and (d).

B. Analysis details

In a moving vehicle scenario, more coils are needed along the vehicle path. While the vehicle is moving, different Tx coils are successively coupled with the Rx. This causes a significant coupling factor oscillation and thus a continuous variation for the condition of maximum power transfer.

Two ways are conceptually feasible to face this problem: i) a standard single coil active at a time [7]; ii) the situation we propose in this paper, with two (or possibly more) coils powered simultaneously.

In the first case, a long movable Rx coil is typically used: the second Tx should be turned on when the first Tx is turned off, and the switch between coils should be done in maximally flat coupling factor conditions. As will be clearer in the results section, the satisfaction of this condition implies a moving coil longer than twice the fixed one, with a consequent reduction of the coupling coefficient and thus a problematic switch between the fixed coils.

In the second case, we propose two coils active at a time: the vehicle is moving above these coils and each coil is turned on and off during the movement. In this case the two active coils can be connected in series or parallel and, since there is a not negligible coupling between the coils, the mutual influence between fixed coils has to be taken into account.

In our numerical approach this is done by considering the system as a 3-port network (in case of 1 Rx and 2 Tx) and by computing its impedance matrix by full-wave simulations. An operating frequency of 6.78 MHz has been assumed in the simulations.

The coupling factor k_{ij} between each couple of coils i and j has then been obtained by equation:

$$k_{ij} = \frac{\left|\mathrm{Im}(Z_{ij})\right|}{\sqrt{\mathrm{Im}(Z_{ii})\,\mathrm{Im}(Z_{jj})}} \tag{1}$$

whereas the conditions imposed by the series or parallel connections of the two Tx coils are satisfied by adopting the following equations, thus reducing the system to an equivalent 2-port network:

$$\begin{aligned} Z_{S11} &= Z_{11} \\ Z_{S12} &= Z_{12} + Z_{13} \\ Z_{S22} &= Z_{22} + Z_{33} + 2Z_{23} \end{aligned} \tag{2}$$

$$\begin{aligned} Z_{P11} &= Z_{11} - \frac{(Z_{12} - Z_{13})^2}{Z_{22} - 2Z_{23} + Z_{33}} \\ Z_{P22} &= \frac{Z_{22}Z_{33} - Z_{23}^{\ 2}}{Z_{22} - 2Z_{23} + Z_{33}} \\ Z_{P12} &= \frac{Z_{12}(Z_{33} - Z_{23}) + Z_{13}(Z_{22} - Z_{23})}{Z_{22} - 2Z_{23} + Z_{33}} \end{aligned} \tag{3}$$

where the subscript S and P stays for series and parallel, respectively. Making use of (1), and assuming that the fixed coil have an identical inductance, the coupling coefficient between the Rx coil and the pair of Tx coils can be derived as

$$k_{S12} = \frac{\sqrt{2}}{2}\frac{k_{12} + k_{13}}{\sqrt{1 + k_{23}}} \tag{4}$$

in the series case and as

$$k_{P12} = (k_{12} + k_{13})\sqrt{\frac{1 - k_{23}}{(1 + k_{23})\left[2(1 - k_{23}) - (k_{12} - k_{13})^2\right]}} \tag{5}$$

in the parallel case.

C. Simulated Results

We start considering the traditional approach of a single Tx active at a time. In Fig. 2 the dependence of the coupling coefficient between coil 1 and 3 (k_{13}) of Fig. 1 is shown as a function of the displacement (normalized with respect to the distance between the centers of the fixed coils).

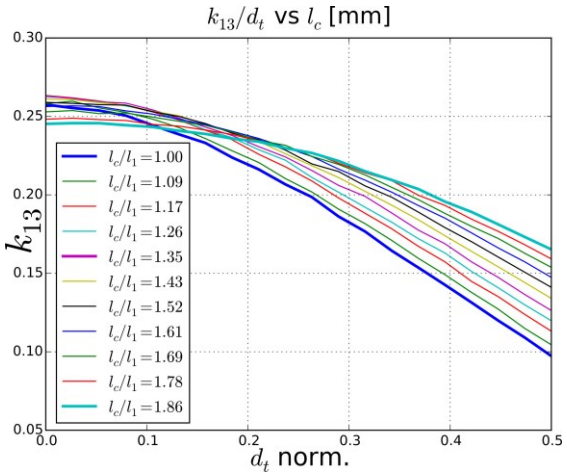

Fig. 2. Coupling factor between coils 1, 3 as a function of displacement d_t.

It can be observed that the coupling coefficient is practically constant when the two inner areas of the inductors are overlying, while it obviously decreases when the shared area is reduced. In this case, the switch between coils 2 and 3 should be done when both coils are in the flat part of the curve, and for this reason the moving coil 1 should be longer than twice the fixed ones. This would make the coupling between the two coils too small and the link less efficient.

The results of the new configuration involving two active Tx coils, obtained by simulations with l_c as design parameter and by applying (2) and (3) in post-processing, are shown in Figs. 3 and 4, for the series and the parallel connection, respectively.

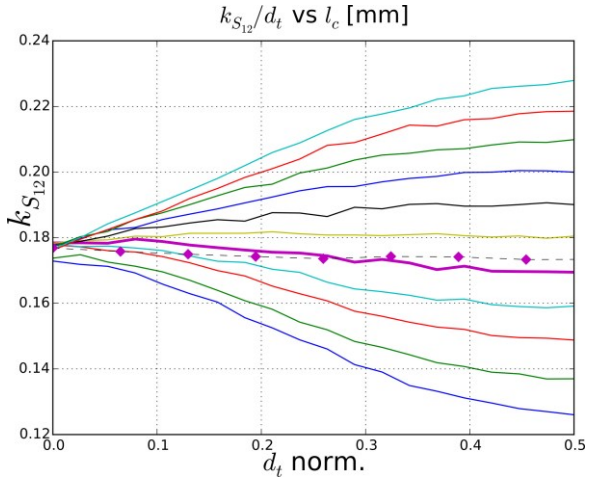

Fig. 3. Coupling factor between moving and both fixed coils with series connection as a function of the displacement d_t. Solid lines: simulated results; diamond markers: measured results.

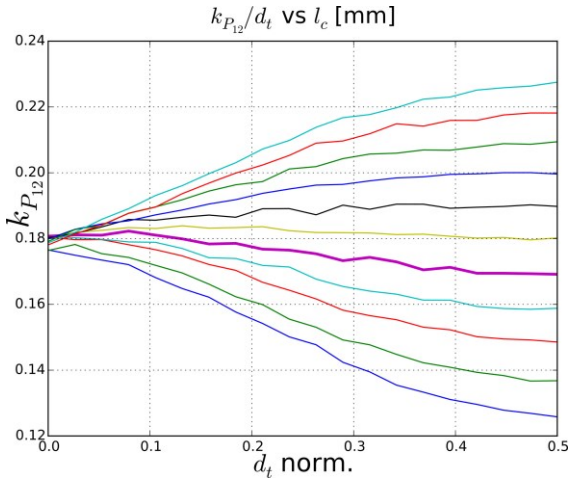

Fig. 4. Simulated coupling factor between moving and both fixed coils with parallel connection as a function of the displacement d_t.

From figures inspection, it is clear that a constant coupling factor between the moving Rx coil and the two fixed Tx coils is guaranteed by a precise topological relationship between the involved coils: in fact, the bold purple line, corresponding to a moving coil normalized length of 1.35 (actually l_c = 159.4 mm), provides the desired flat behavior in both the configurations. In particular, referring to parameters definition of Fig. 1, the condition on the inner length of the moving coil suggested by experiments can be cast in the following way:

$$l_c = l_1 + \frac{(l_2 - l_1)}{2} + d_c \tag{6}$$

A qualitative explanation can be given by considering some simplifying hypotheses: we need to consider a uniform magnetic field inside each turn of the coils and negligible outside, as is for an infinitely long inductor. The total flux is thus obtained by considering just the sum of the fluxes. The involved area for each of these fluxes is the intersection area between each turn of the moving coil and each turn of both fixed coils. By supposing both coils to have the same magnetic field, with l_c given by (6), the variation of the shared flux (and consequently of the coupling factor) is minimized.

For the series connection we also provide measured data of the flattest case, which are in good agreement with the simulated ones and marked by diamonds (Fig. 3).

It is worth noting that the described behavior is almost identical for both the series and the parallel connections. However a deeper inspection of the results of Figs. 3 and 4 reveals that the value of k_{S12} and k_{P12} are identical only when the Rx coil is midway between the Tx coils, and that the difference between the coupling factors increases as the center of the Rx coil gets closer to the center of one of the fixed coils. In particular, for $d_t = 0$ the values of k_{S12} and k_{P12} are 0.181 and 0.183, respectively.

This result is in accordance with the expressions of the coupling coefficients (4) and (5). As a matter of fact, for $d_t = 0.5$ the couplings between the Rx and each of the Tx coils are identical ($k_{12} = k_{13}$) and in these condition (4) and (5) provide the same result. On the other hand, for $d_t = 0$ (or equivalently for $d_t = 1$) the difference between the coupling factors is maximum and this also maximizes the value of k_{P12} given by (5).

This behavior can also be explained by considering that for $k_{12} \neq k_{13}$ the currents in the two coils connected in parallel, assume different values due to the effect of the load drain. The primary consequence of this unbalance is an increase of the current in the aligned fixed coil and thus a decrease of the total dispersed flux and a consequent increase of k_{P12} in the aligned case.

All the described behaviors can be reproduced by scaling the whole structure, thus enabling a single structure to be used for different applications. In this case, attention should be anyway kept to avoid issues due to parasitic effects: the frequency should be chosen where the imaginary part of the impedance is approximately linear. In this way, we can reasonably consider to be far from problems related to the parasitic resonance.

III. CONCLUSION

A new idea enabling constant coupling in moving resonant WPT systems has been proposed in this paper. According to this idea and referring to electrical vehicle applications, a series of Tx coils should be disposed along the vehicle path and a couple of them should be simultaneously activated while the vehicle is moving over them.

While the vehicle moves between the active coils the coupling coefficient is practically constant. Every time the Rx coil aligns with one of the Tx coils the coil which precedes is activated and the coil which follows is deactivated.

The system behavior is thus periodic and the coupling coefficient can be kept constant along all the vehicle path, thus making easier the fulfilment of conditions such as the maximum power transfer.

Measured data of the best configuration are in good agreement with predicted ones.

ACKNOWLEDGMENT

This work was partly funded by the financial Support of the European Commission, within the framework of the ARTEMIS ARROWHEAD project

REFERENCES

[1] A. Costanzo, M. Dionigi, F. Mastri, M. Mongiardo, J. A. Russer and P. Russer, "Rigorous network modeling of magnetic-resonant wireless power transfer", Wireless Power Transfer Journal, vol. 1, no. 1, pp 27-34, Mar. 2014.

[2] M. Fu, T. Zhang, C. Ma, and X. Zhu, "Efficiency and Optimal Loads Analysis for Multiple-Receiver Wireless Power Transfer Systems," IEEE Trans. Microwave Theory Tech., vol. 63, no.3, pp. 801–812, Mar. 2015.

[3] A. P. Sample, D. A. Meyer, and J. R. Smith, "Analysis, experimental results, and range adaptation of magnetically coupled resonators for wireless power transfer," IEEE Trans. Ind. Electron., vol. 58, no. 2, pp. 544–554, Feb. 2011

[4] C. Florian, F. Mastri, R. Paganelli, D. Masotti, and A. Costanzo, "Theoretical and numerical design of a wireless power transmission link with GaN-based transmitter and adaptive receiver," IEEE Trans. Microwave Theory Tech., vol. 62, no. 4, pp. 931–946, April 2014.

[5] J. Kim, H.-C. Son, D.-H. Kim, K.-H. Kim, and Y.-J. Park, "Efficiency of magnetic resonance WPT with two off axis self-resonators," IEEE MTT-S International Microwave Workshop Series on Innovative Wireless Power Transmission: Technologies, Systems, and Applications (IMWS), May 12–13, 2011, pp. 127–130.

[6] T. C. Beh, M. Kato, T. Imura, S. Oh, and Y. Hori, "Automated impedance matching system for robust wireless power transfer via magnetic resonance coupling," IEEE Trans. Ind. Electron., vol. 60, no. 9, pp. 3689–3698, Sep. 2013.

[7] J. A. Russer, P. Russer, "Design considerations for a moving field inductive power transfer system," in IEEE Int. Wireles Power Transfer Conf. (WPTC), May15 - 16 2013, pp. 147 - 150.

[8] J. A. Russer, M. Dionigi, M. Mongiardo, and P. Russer, "A moving field inductive power transfer system for electric vehicles," in Proc. European Microwave Conf.(EuMC), Oct. 6-11 2013, pp. 519–522.